

Splay Faults in the Makran Subduction Zone and Changes of their Transferred Coulomb Stress

Hosseini Mehr, A.¹, Maleki Asayesh, B.^{2*} and Mokhtari, M.³

1. M.Sc. Geophysics, Department of engineering, Islamic Azad university Marivan branch, Marivan, Iran

2. Ph.D. Student, International Institute of Earthquake Engineering and Seismology (IIEES), Tehran, Iran

3. Assistant Professor, Department of Seismology, International Institute of Earthquake Engineering and seismology(IIEES), Tehran, Iran

(Received: 18 Nov 2015, Accepted: 23 May 2017)

Abstract

The Makran subduction zone in northeast and the Sumatra subduction zone (Sunda) in the west have been known as tsunamigenic zones of the Indian Ocean. The 990 km long Makran subduction zone is located offshore of Iran, Pakistan and Oman. Similar to many subduction zones all over the world, the Makran accretionary prism is associated with an imbricate of thrust faults across the zone, which may rupture due to great earthquakes. Based on some studies, it has been suggested that the presence of young marine terraces along parts of the western Makran, Jask, and Konarak, providing a strong evidence for the occurrence of great thrust earthquakes in the western Makran. Besides, this region might have experienced a strong earthquake in 1483 (Mw=7.2). This study uses 2D seismic reflection data to map the splay faults in the western Makran subduction zone. The result of this interpretation has been presented on map showing the major splay and normal faults, in the south and north, respectively. Furthermore, Coulomb stress changes is calculated along the splay faults, following a hypothetical earthquake (Mw=7.2) on the megathrust. The amount of slip that transfers from the plate boundary onto the splay faults during large subduction earthquake and the pattern of slip partitioning between them are calculated. The results show that the slip on Megathrust increases stress in some parts of surrounding areas. Some splay faults are located in these areas that can be loaded in shallow depth and are likely the sources of aftershocks. Since the slip on splay faults has a key significance in generating tsunami, their analysis is an important issue in tsunami risk assessment. It is strongly suggested that the result of this study is used as an input parameter for a comprehensive tsunami hazard modeling in the Makran region.

Keywords: Subduction zone, Splay faults, Seismic reflection data, Coulomb stress changes.

1. Introduction

The 990 Km long Makran subduction zone is located offshore of Iran, Pakistan and Oman (Mokhtari et al., 2008).

By using 2D seismic reflection data, we map and interpret the splay faults in the western Makran region located on the Iranian territory. Splay faults are common features in most accretionary prisms, growing as sediments are added from the upper plate. These thrust faults in accretionary prisms may rupture due to the great subduction zone earthquakes (Sykes and Menke, 2006). Splay faults are also known as secondary tsunami sources and have been responsible for a large part of tsunami losses during the tsunamis occurred in the past (Cummins and Kaneda, 2000).

Previous studies showed that the occurrence

of an earthquake can affect the faults that located in the surrounding area and by loading them, brought them to the failure condition. Therefore, key features of thrust earthquake triggering, inhibition, and clustering can be explained by Coulomb stress changes. The slip on blind thrust faults increases the stress on some nearby zones, particularly above the source fault. Blind thrusts can thus trigger the slip on secondary faults at shallow depth and typically produce broadly distributed aftershocks (King et al., 1994; Lin and Stein, 2004). Based on Lin and Stein (2004), subduction zone ruptures are calculated to promote normal faulting events in the outer rise and to promote thrust-faulting events on the periphery of the seismic rupture and its downdip extension.

*Corresponding author:

b.m.asayesh@gmail.com

Thus, the occurrence of an earthquake on the megathrust could transfer stress on the splay faults where known as secondary tsunami sources.

This study interprets the seismic profiles indicated on Figure 1 and map the splay faults along the western Makran. Then, Coulomb stress changes and its effects on splay faults based on a hypothetical earthquake ($M_w=7.2$) in this region is calculated in order to assess the transferred stress on the surrounding faults.

2. Tectonic and seismotectonic setting of the Makran Accretionary Prism

The east-west trending Makran Subduction zone with 990 km length is located offshore of Iran, Pakistan and Oman. The Makran subduction zone marks a zone of convergence where the oceanic crust of the Oman Sea is subducting beneath the Eurasian continental plate since early Cretaceous (Farhoudi and Karig, 1977). The Plate Boundaries in Makran region are: (i) The Zendan-Minab Fault System that represents the eastern boundary of the Arabian Plate (Figure 1), (ii) the Oranch Fault Zone that is part of the Eurasian-Indian plate boundary complex (Figure 1), and (iii) the NE-SW trending Murray Ridge System in the northern Arabian Sea extends for about 750 km.

Unlike most of the other accretionary complexes in the world, there is no obvious trench developed in front of the Makran Accretionary Complex (Mokhtari et al., 2008). The absence of trench in this region can be due to the fact that the subduction angle at the accretionary front is very low that could be due to the existence of thick sediments with low compaction or it might be caused by high deposition rate. It seems that the first reason may be more plausible.

The rate of convergence along the Makran boundary increases slightly from the west

towards the east (DeMets et al., 1990). Average Convergence rate in the Makran subduction zone is about 4 cm/yr that increases from 3.65 cm/yr in west to 4.2 in the east. Moreover, GPS measurements suggest that the lowest subduction rate of Oman plate beneath the Eurasian plate occurs in the west at about 1.95 cm/yr while the highest rate occurs at about 2.7 cm/yr in the east (Vernant et al., 2004). Based on Zarifi (2006), the direction of compressional stress axis is rotating along the Makran subduction zone. The western Makran stress field is under the influence of the collision between Arabia and Eurasia, while the eastern Makran stress field is affected by Indian-Eurasian collision. The Makran subduction zone exhibits a strong segmentation between east and west in its seismic behavior. The plate boundary in eastern Makran has ruptured in large and great thrust earthquake of 1945 and currently experiences small- and moderate-sized thrust earthquakes. On the contrary, western Makran exhibits no well-documented great earthquakes in historic times, and modern instrumentations are not detecting any shallow events along the plate boundary (Byrne et al., 1992).

The present-day Makran accretionary prism located in offshore part of Iran has almost a triangular wedge geometry (Figures 2, 3 and 4), and displays active thrust faults. The main phase of deformation of the imbricate fan at the front of the Makran accretionary prism occurred during the Late Miocene to Late Pliocene (Grando and McClay, 2007). The present day geometry of the seabed indicates that most of the fault-propagation folds are still active, and displayed surface topography on the seabed, suggesting that the accretionary prisms is suffering from the current deformations. Based on Grando and McClay (2007), since the Pliocene-Pleistocene, the coastal Makran and the mid-slope area have experienced uplift, normal faulting and ductile flows.

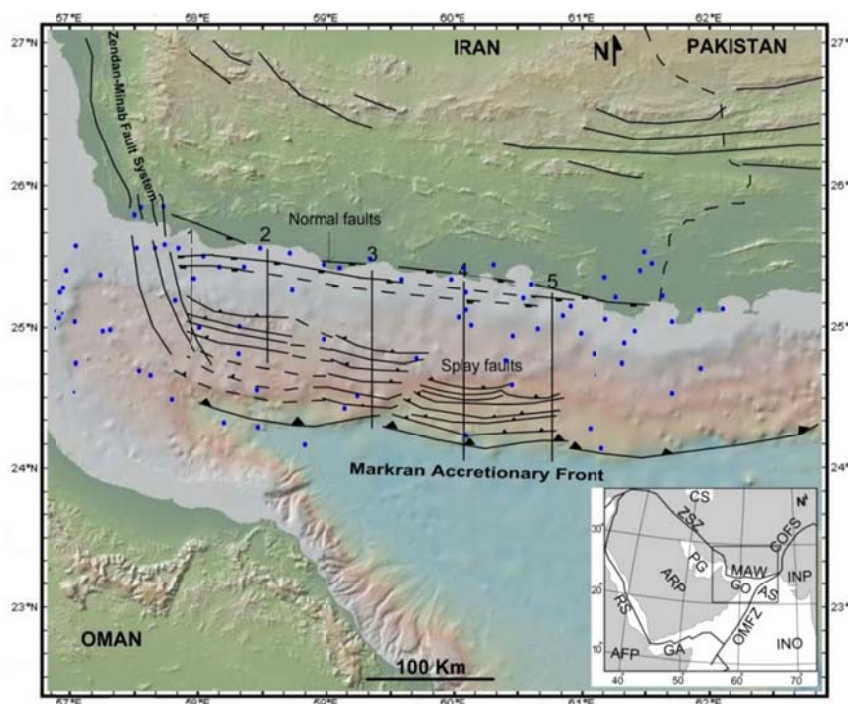


Figure 1. Generalized map of the Makran subduction zone. The blue dots show earthquake epicenters. Straight lines numbered 1-5 are the seismic lines. Solid lines indicate faults in western Makran. Abbreviations on the inset: AFP; African Plate, ARP; Arabian Plate, AS; Arabian Sea, COFS; Chaman Oranch Fault System, CS; Caspian Sea, GA; Gulf of Aden, GO; Gulf of Oman, INO; Indian Ocean, INP; Indian Plate, MAW; Makran Accretionary Wedge, OMFZ; Owen Murray Fault Zone, PG; Persian Gulf, RS; Red Sea, ZSZ; Zagros Suture Zone.

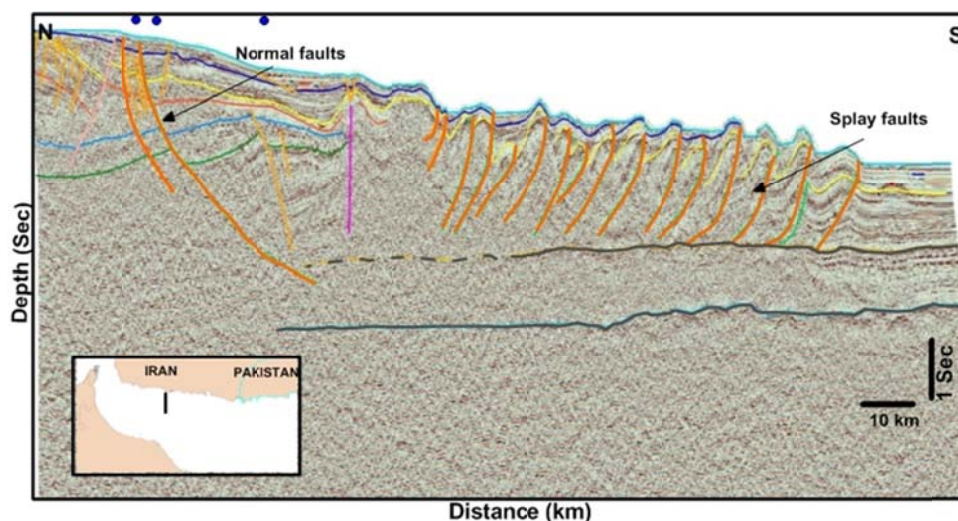


Figure 2. Seismic profile (line 5) across the western sector of the Makran accretionary prism. Splay faults (right) and Normal faults (left) are interpreted and overlain on the profile. Blue dots indicate epicenters of three earthquakes. The location of seismic profile is shown on the inset (see also Figure 1 for location). Some bedding planes are also shown in colored lines to help interpretations.

3. Data and methodology

In this study, 2-D seismic data are used to interpret splay faults distributed along and across the western Makran. These seismic

profiles gathered under auspices of National Iranian Oil Company in 2000 using conventional marine 2D seismic methodology. These are part of

PC2000 project that covers both the Persian Gulf and Oman Sea. These data are interpreted using 'SMT' seismic interpreting data package. Seismic earthquake data are collected from the International Institute of Earthquake Engineering and Seismology (IIEES) and International Seismological Center (ISC). Unfortunately, due to seismic network without adequate azimuth, these earthquake data have uncertainty of locations and depth.

In order to compute Coulomb stress changes, we assume the occurrence of an earthquake of $M_w=7.2$ in the region. We need to remind that the occurrence of such a hypothetical event is quite plausible considering the historical seismicity in the eastern Makran and the tectonic setting of the Makran subduction zone.

4. Identified faults and their seismicity

We recognized several faults in the study area (see Figures 1, 2, 3 and 4). These faults can be generally divided into two groups. The first group is splay faults that are thrust and begin from trench side in the south where that indicates the front of the accretionary prism and continues northward to the Makran coast. The second group is normal faults that are located far behind the front along the Makran coast. Some of the splay faults cut two horizons that interpreted as seafloor and bottom simulating reflector. However, many of them have not reached the seafloor and only affected the Pliocene Makran sands (Figures 2, 3 and 4). Previous studies indicate that since the Pliocene–Pleistocene times the coastal Makran and the mid-slope area have experienced uplift, normal faulting and

ductile flow (Grando and McClay, 2007). As the horizontal distances between seismic profiles are large, the horizontal extension of faults due to the uncertainty has been shown by dashed lines. However, it is important to mention that despite this, the splay faults that have been shown in the map can be used with an acceptable resolution for the future tsunami hazard assessment purposes.

It has long been known that splay faults exist in most subduction zones (Sykes and Menke, 2006; Ryan and Scholl, 1989). According to Sykes and Menke (2006), splay faults are common in most modern accretionary prisms, which grow as sediments are added from the upper plate. The sediment with high volume can be a suitable place for the growth of splay faults (Figures 2, 3 and 4). These thrust faults in accretionary prisms may be ruptured due to the great earthquakes in subduction zone.

The present day seismicity in Makran is sparse. Moderate to large magnitude earthquakes are either related to the down going slab at intermediate depths or superficial in the eastern Makran (e.g. 1765, 1851 and 1945 earthquakes), while western Makran is marked with almost no high seismicity in the coastal area at present, but might have experienced a strong earthquake in 1483 (Ambraseys and Melville, 1982; Byrne et al., 1992). Furthermore, Page et al. (1979) have suggested that the presence of young marine terraces along parts of the western Makran, Jask, and Konarak are providing a strong evidence for the occurrence of great thrust earthquakes in the western Makran.

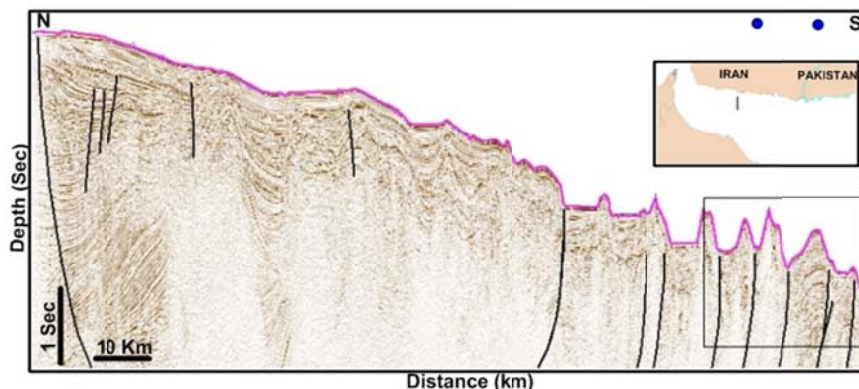


Figure 3. Seismic profile (line 4) across the western sector of the Makran accretionary prism. Splay faults (right) and Normal faults (left) are shown. Blue circles indicate occurred earthquakes in the region. The location of seismic profile is shown on the right up and also in Figure 1.

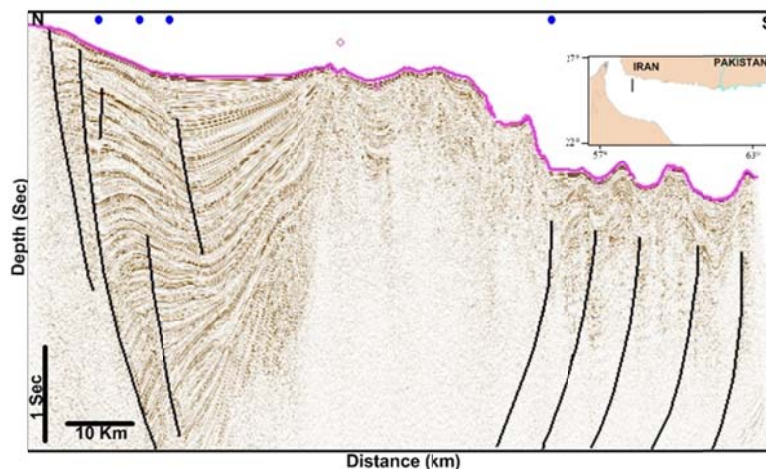


Figure 4. Seismic profile (line 1) across the western sector of the Makran accretionary prism. Splay faults (right) and Normal faults (left) are shown. Blue circles are occurred earthquakes. The location of seismic profile is shown in right up and also in Figure 1.

5. Coulomb Failure Stress Changes

Based on King et al. (1994) various criteria have been used to characterize the conditions under which failure occurs in rocks. One of the more widely used is the Coulomb failure criterion. The Coulomb stress change ΔCFF is defined by:

$$\Delta CFF = \Delta\tau - \mu(\Delta\sigma_n - \Delta P) \quad (1)$$

where ΔCFF is the change in failure stress on the receiver fault caused by slip on the source fault(s), $\Delta\tau$ is the change in shear stress on the receiver fault (reckoned positive when sheared in the direction of fault slip), $\Delta\sigma_n$ is change in normal stress acting on the receiver fault (positive if the fault is unclamped), ΔP is the pore fluid pressure (positive in extension), and μ is the friction coefficient (Mouyen et al., 2010; Parsons et al., 1999). Pore fluid pressure modifies the effective normal stress across the failure plane, as shown in Equation (1), so with introducing the effective coefficient of friction $\mu' = \mu(1 - B)$, in which B is the Skempton coefficient (that varies from 0 to 1) (King et al., 1994; Mouyen et al., 2010; Cattin et al., 2009), we will have:

$$\Delta CFF = \Delta\tau - \mu'\Delta\sigma_n \quad (2)$$

The Skempton coefficient links the change in pore pressure to the change in normal stress. For a detailed description of ΔCFF computation, see Cattin et al. (2009).

Following Parsons et al. (1999) we tend to assume a high coefficient of friction (~ 0.8)

for continental thrust faults, moderate friction (0.4) for strike-slip or unknown faults, and very low friction (>0.2) for major transforms, such as the San Andreas fault. The correspondence between the off-fault aftershocks and the calculated unclamping for the Whittier Narrows earthquake suggests that the aftershocks of thrust faults are sensitive to normal stress changes. Thus, the apparent friction coefficient, μ' , in the Coulomb stress equation would appear to be high for thrust faults, perhaps about 0.8. This inference has also been made for other thrusts and for strike-slip faults with little cumulative slip, perhaps because youthful fault surfaces are rough (Parsons et al., 1999; Toda and Stein, 2003).

6. Discussion

6.1. Pre-stress state and angle between the main and the branching faults

Kame et al. (2003) suggested that the tendency of a fault to branch depends on three parameters:

- 1) The orientation of the local pre-stress field (S_{max})
- 2) The rupture velocity
- 3) The angle between the main and the branching faults.

The processes of shear stress build up in the contact zone in Makran subduction zone is very slow (Zarifi, 2006). It takes almost 1400 years until the shear stress in the strongly coupled part of the slab interface reaches the yield point (Zarifi, 2006). However, this

calculation cannot be the representative of the recurrence time for an earthquake, since it did not consider any complexity regarding the frictional behavior, preexisting stress or loading due to the occurrence of other earthquakes in this segment of subduction. We have measured dip angles from the one post stack depth migrated profile shown in Figure 2 (Line No 5 in Figure 1). We determine that the branching angle of the splay had the range of $\varphi = 15^\circ$ to 35° , with average of 25° . Assuming that the principal precompression is horizontal, we can equate Ψ to the slope of the plate interface at the junction where the splay branches off into the sedimentary wedge, again, depending on profile No 5, that gives $\Psi = 7^\circ$. Thus, this case is closest to Figure 5, first and second rows of panels,

although Ψ is somewhat smaller in the simulations shown there. Splay faults with sharper dip ($\varphi = 35^\circ$) are located at the front of the accretionary prism. Inner splay faults show shallower angles. Simultaneous rupture propagation on both faults (megathrust and splay faults) after bifurcation will be more difficult for smaller branching angle due to the stress interaction that suppresses rupture on the other fault through stress shadowing.

When rupture velocity is low, off-fault stressing is not high enough to continue rupture on the branching fault and the weak stress shadowing from the main fault prevails. As rupture velocity increases, off-fault stresses are enhanced so that the rupture on the branching fault can continue to propagate indefinitely (Figure 5).

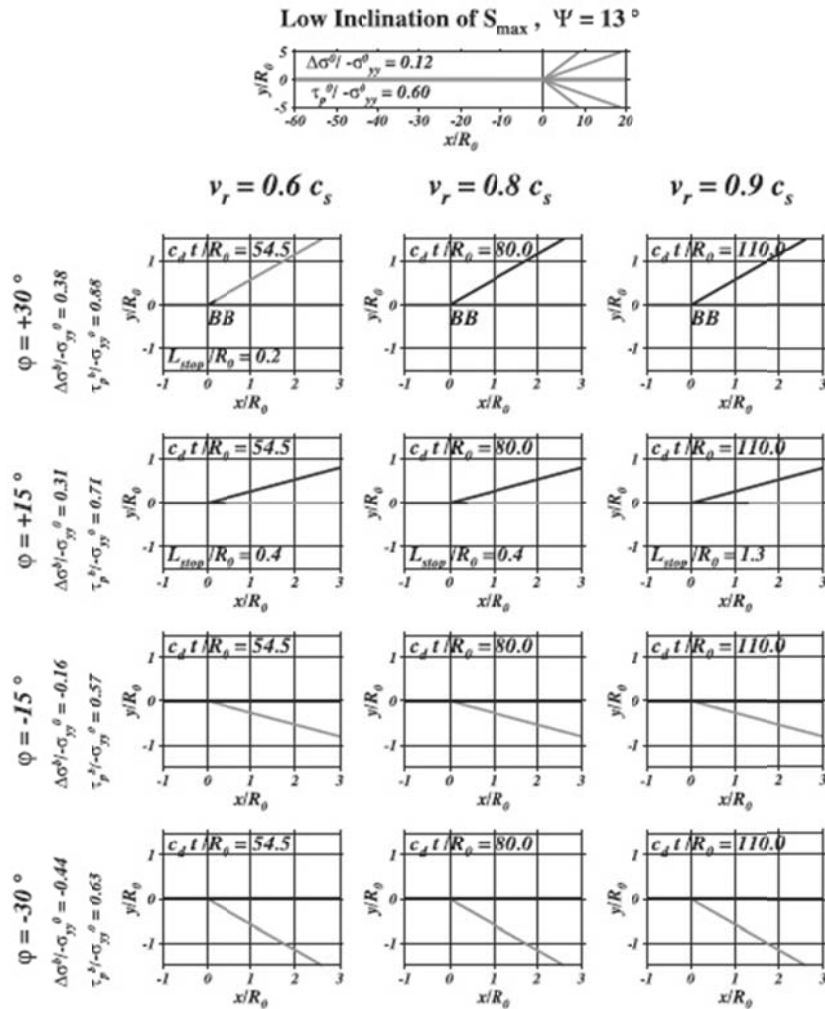


Figure 5. Diagram of final rupture traces in the vicinity of the intersection for cases with low inclination of S_{max} , $\Psi = 13^\circ$. L_{stop} indicates the length of arrested rupture once dynamically nucleated. BB indicates branching behind (Kame et al., 2003).

Among other parameters, it will be important to know the pre-stress state along the fault system and, particularly, principal directions near any branching junctions. These stress directions should include not only the regional tectonic stress field, but also the effects from previous earthquakes on the fault system, which may cause strong local deviations from the larger-scale stress field (Kame et al., 2003).

Fukao (1979) indicated that rupture propagation onto splay faults within accretionary wedges is one of the main mechanisms for generating large tsunamis. In fact, different studies have shown that the total slip during a large megathrust earthquake can be partitioned between the subduction-zone plate boundary and splay faults within the accretionary wedge (e.g., Baba et al., 2006). The amount of slip that transfers from the plate boundary onto splay faults during large subduction earthquakes and the pattern of slip partitioning between them can be an important issue in view of tsunami hazard assessment, because the seafloor uplift due to splay faults is relatively larger, resulting in large tsunamis.

6.2. Coulomb stress changes due to hypothetical earthquake along the Makran megathrust

As mentioned in the previous sections, splay faults are known as secondary tsunami sources, and most of the moderate to large aftershocks usually occur on them. After a

large earthquake on the megathrust, it will be possible that splay faults to be loaded and cause moderate or large aftershocks and consequently moderate or large tsunamis. For investigation of transferred stress due to the occurred earthquakes on megathrust fault in surrounding area specially on splay faults, we attribute an earthquake with magnitude $M_w=7.2$ to the megathrust fault and then calculate the stress change due to this earthquake on splay faults. Occurrence of an earthquake with this magnitude are possible based on historical evidences and studies (Ambraseys and Melville, 1982; Byrne et al., 1992; Page et al., 1979). Table (1) shows the characteristics of this earthquake. By using well-known relations in Wells and Coppersmith (1994) and Hanks and Kanamory (1979), we calculate length, width, moment and displacement for this hypothetical earthquake (Table 2).

Based on data from Tables (1) and (2) and modeling parameters that are summarized in Table (3), we calculated Coulomb stress changes on splay faults as receiver faults (for $\mu'=0.4$ and $\mu'=0.8$), and results are shown respectively (Figures 6 and 7). As argued before, using 0.8 as a friction coefficient in the subduction zones has a reliable result. However, we used both 0.4 and 0.8 as a friction coefficient to compare the results, and we observed that for $\mu'=0.8$ the off-fault lobes of stress change in cross-sections are larger than end-fault lobes (Figures 6 and 7).

Table 1. Source parameters for assumed earthquake.

Lat.	Lon.	Depth (km)	Magnitude (M_w)	Azimuth	Dip	Rake
24.77	58.80	10	7.2	270	7	90

Table 2. Length, width, moment and slip for this hypothetical earthquake by using well-known relations in Wells and Coppersmith (1994) and Hanks and Kanamory (1970, 1979).

Length (km)	57
Width (km)	22
Area (km^2)	1254
Moment ($*10^{18}$)N.M	0.708
Minimum Slip (m)	0.8
Maximum Slip (m)	1.77
Mean Slip (m) (used for calculation)	1.25

Table 3. Modeling parameters for computing ΔCFF .

Poisson ratio	0.25
Shear modulus	300,000 bar
Grid size	1km
Friction coefficient (μ')	0.4&0.8
Target planes (strike/dip/rake)	270/35/90

In Figures 6 and 7, we consider that the slip on megathrust increases stress on surrounding areas. Therefore, slip on thrust faults can trigger slip on secondary faults at shallow depth such as splay faults that are located in the increased stress zones. Our calculation in this study shows that the slip on megathrust enhances stress in areas where there are both normal and thrust faults.

Hence, we can conclude that after occurring hypothetical slip on megathrust, the occurrence of aftershocks with normal and rivers mechanisms along splay faults are possible. Accordingly, it can be considered as a hazard, because they occur in the shallow splay faults first and also have capability to cause tsunami.

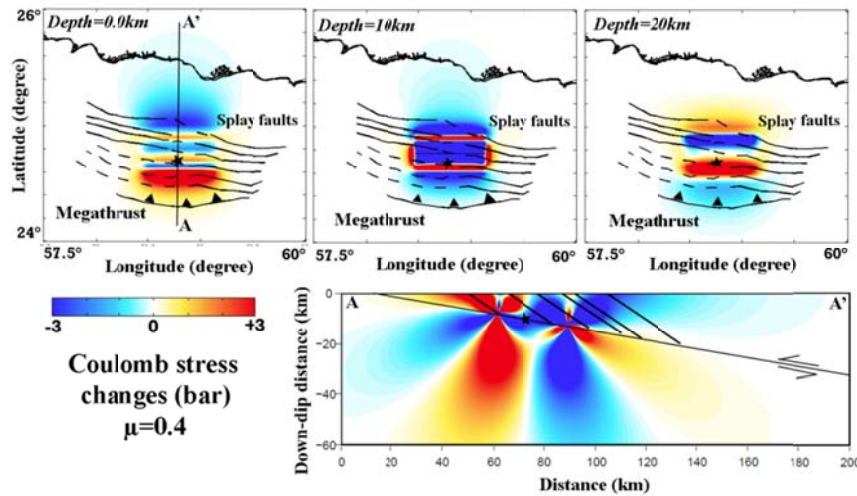


Figure 6. Coulomb stress changes due to the hypothetical earthquake ($M_w=7.2$) assumed at depth of 10 km for $\mu'=0.4$. Top three map views show stress change at three different depth (0, 10, 20 Km). Cross section along the AA' profile are shown at bottom right-hand. Megathrust and Splay faults are shown in all map views. Locations of the hypothetical earthquake are shown with black star.

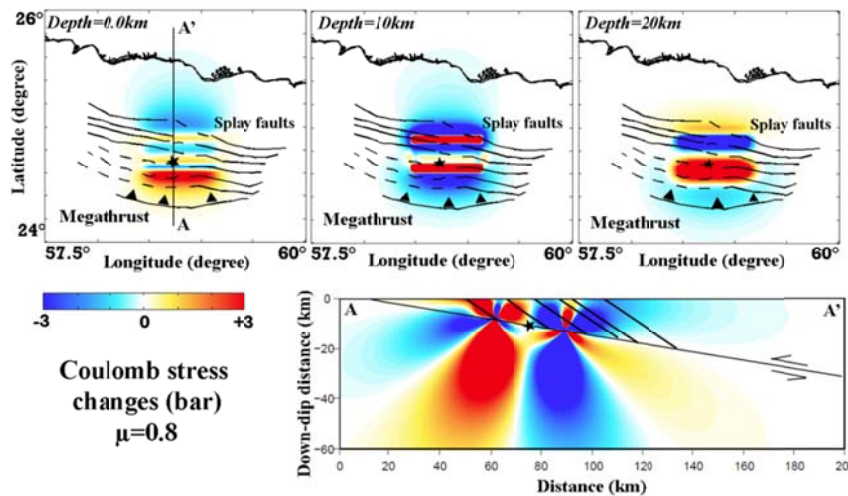


Figure 7. Coulomb stress changes due to hypothetical earthquake ($M_w=7.2$) assumed at depth of 10 km for $\mu'=0.8$. Top three map views show stress change at three different depth (0, 10, 20 Km). Cross section along the AA' profile are shown at bottom right-hand. Megathrust and Splay faults are shown in all map views. Locations of the hypothetical earthquake are shown with black star.

7. Conclusions

Earthquakes that occur in subduction zones are so important because the largest earthquakes occur in this region and they can cause tsunamis. Identifying of splay faults in the subduction zones will be useful because of seismic hazard and tsunami hazard. These faults based on studies conducted elsewhere on the other subduction zones have been indicated as a major contributor for tsunami strengthening factor mainly in local sense. We used seismic data and distribution of earthquakes in the Makran to identify splay faults in this region. These seismic data have been utilized in mapping the splay faults in the western Makran region about which we do not have enough knowledge because of less earthquake data. We have measured the branching angle of the splay faults. They have the range $\varphi = 15^\circ$ to 35° , with average of 25° and $\Psi = 7^\circ$. Splay faults with sharper dip ($\varphi = 35^\circ$) are located at the front of the accretionary prism, and inner splay faults show gentle angles. These angles can be used in simulations of final rupture traces in the vicinity of the intersection and other studies about tsunami hazard modeling.

In order to investigate the effect of large earthquake due to megathrust fault in the splay faults, we calculated the Coulomb stress changes due to a hypothetical earthquake that can occur in this fault. Our calculation showed that the transferred stress due to the hypothetical earthquake can affect the splay faults and at some parts of these splay faults that are located in front of the accretionary prism, and have sharp angles, the coulomb stress changes are positive. Therefore, after occurring of an earthquake along the megathrust, some parts of these splay faults are loaded and are the most vulnerable places for aftershocks and future events. Because these splay faults can be assumed as the secondary sources of tsunami, it is strongly recommended that these faults, their angle, and patterns of distributed Coulomb stress changes on them to be included for a more comprehensive tsunami hazard modeling.

Acknowledgements

The authors would like to thank Dr. K. Hessami (from IIEES) for suggestions which led to the improvement of this manuscript.

The authors would also like to thank National Iranian Oil Company, Exploration Directorate for providing the seismic sections and permission for their publication.

References

- Ambraseys, N. and Melville, C., 1982, *A History of Persian Earthquakes*. Cambridge University Press, New York.
- Baba, T., Cummins, Ph. R., Hori, T., and Kaneda, Y., 2006, High precision slip distribution of the 1944 Tonankai earthquake inferred from tsunami waveforms: Possible slip on a splay fault, *Tectonophysics*, 426, 119–134, doi:10.1016/j.tecto.2006.02.015.
- Byrne, D. E., Sykes, L. R., and Davis, D. M., 1992, Great thrust earthquakes and a seismic slip along the plate boundary of the Makran subduction zone. *J. Geophys. Res.*, 97, 449–478.
- Cummins, Ph. R. and Kaneda, Y., 2000, Possible splay fault slip during the 1946 Nankai earthquake. *Geophysical Research Letters*, 27, 17, 2725–2728.
- Cattin, R., Chamot-Rooke, N., Pubellier, M., Rabaute, A., Delescluse, M., Vigny, C., Fleitout, L. and Dubernet, P., 2009, Stress change and effective friction coefficient along the Sumatra-Andaman-Sagaing fault system after the 26 December 2004 ($M_w = 9.2$) and the 28 March 2005 ($M_w = 8.7$) earthquakes, *AGU and the Geochemical Society*, 10(3), Q03011, doi:10.1029/2008GC002167 ISSN: 1525-2027.
- De Mets, C., Gordon, R. G., Argus, D. F. and Stein, S., 1990, Current plate motions. *Geophys. J. Int.*, 101, 425–478.
- Farhoudi, G. and Karig, D. E., 1977, The Makran of Iran and Pakistan as an Active Arc System. *Abstr., EOS Trans., Am. Geophys. Union.*, 58, 446.
- Grando, G. and McClay, K., 2007, Morphotectonics domains and structural styles in the Makran accretionary prism, offshore Iran. *Sedimentary Geology*, 196, 157–179.
- Hanks, T. C. and Kanamori, H., 1979, A moment magnitude scale, *Journal of Geophysical Research*, 84, 2348–2350.
- Kame, N., Rice, J. R. and Dmowska, R., 2003, Effects of prestress state and rupture velocity on the energy release in

- great earthquakes. *Journal of Geophysical Research*, *Journal of Geophysical Research*, 84, 2303–2314.
- King, G. C. P., Stein, R. S. and Lin, J., 1994, Static stress changes and the triggering earthquakes, *Bull. Seismol. Soc. Am.*, 84(3), 935–953.
- Lin, J. and Stein, R. S., 2004, Stress triggering in thrust and subduction earthquakes and stress interaction between the southern San Andreas and nearby thrust and strike-slip faults. *Journal of Geophysical Research*, Vol. B02303, doi:10.1029/2003JB002607.
- Mokhtari, M., Abdollahie Fard, I. and Khaled Hessami, H., 2008, Structural elements of the Makran region, Oman sea and their potential relevance to tsunamigenesis. *Natural Hazards*, 47, 185–199.
- Mouyen, M., Cattin, R. and Masson, F., 2010, Seismic cycle stress change in western Taiwan over the last 270 years. *Geophysical Research Letters*, 37(3).
- Page, W. D., Alt, J. N., Cluff, L. S. and Plafker, G., 1979, Evidence for the recurrence of large magnitude earthquakes along the Makran coast of Iran and Pakistan. *Tectonophysics*, 52, 533–547.
- Parsons, T., Stein, R. S., Simpson, R. W. and Reasenberg, P. A., 1999, Stress sensitivity of fault seismicity: A comparison between limited-offset oblique and major strike-slip faults, *J. Geophys. Res.*, 104, 20,183–20,202.
- Ryan, H. F. and Scholl, D. W., 1989, The evolution of forearc structures along an oblique convergent margin, central Aleutian Arc. *Tectonics*, 8, 497–516.
- Sykes, L. R. and Menke, W., 2006, Repeat times of large earthquakes: implications for earthquake mechanics, *Bulletin of the Seismological Society of America*, 96, 5, 1569–1596.
- Toda, S. and Stein, R. S., 2003, Toggling of seismicity by the 1997 Kagoshima earthquake couplet: A demonstration of time-dependent stress transfer, *J. Geophys. Res.*, 108(B12), 2567, doi:10.1029/2003JB002527.
- Vernant, P., Nilforoushan, F., Hatzfeld, D., Abbassi, M. R., Vigny, C., Masson, F., Nankali, H., Martinod, J., Ashtiani, A., Bayer, R., Tavakoli, F. and Ch'ery, J., 2004, Contemporary crustal deformation and plate kinematics in the Middle East constrained by GPS measurements in Iran and Northern Oman, *Geophys. J. Int.*, 157, 381–398.
- Wells, D. L. and Coppersmith, K. J., 1994, New empirical relationships among magnitude, rupture length, rupture width, rupture area, and surface displacement. *Bulletin of the Seismological Society of America*, 84.
- Zarifi Z., 2006, Unusual subduction zones: case studies in Colombia and Iran, Unpublished Ph.D. Thesis., University of Bergen, Norway.